

Supplemental Information

**Engineering Activatable Promoters for
Scalable and Multi-Input CRISPRa/i Circuits**

Diego Alba Burbano^{+,1,4}, Ryan A.L. Cardiff^{+,2,4}, Benjamin I. Tickman^{2,4}, Cholpisit Kiattisewee^{2,4}, Cassandra J. Maranas^{2,4}, Jesse G. Zalatan^{*,2,3,4}, James M. Carothers^{*,1,2,4}

1: Department of Chemical Engineering
University of Washington
Seattle, WA 98195
United States

2: Molecular Engineering & Sciences Institute
University of Washington
Seattle, WA 98195
United States

3: Department of Chemistry
University of Washington
Seattle, WA 98195
United States

4: Center for Synthetic Biology
University of Washington
Seattle, WA 98195
United States

+: These authors contributed equally

*: Corresponding authors
zalatan@uw.edu
206-543-1670

jcaroth@uw.edu
206-221-4902

In preparation as an article for *Proc. Natl. Acad. Sci. USA*

Supplementary Figures

Figure S1: Minimal promoter effect on fold-change

Figure S2: UP-element libraries RFP distributions

Figure S3: UP-element libraries fold-change distributions

Figure S4: CRISPRa activity validation of high GC-content scRNAs

Figure S5: Combinatorial construction of activatable promoters

Figure S6: Activatable promoter characterization in CFS

Figure S7: scRNA dose-response characterizations

Figure S8: Titration of middle node in two-layer activation cascade

Figure S9: Signal propagation in a two-layer activation cascade

Figure S10: Time course for four-layer activation cascade assembly strategies

Figure S11: Four-layer activation cascade basal and activated RFP expression

Figure S12: Signal propagation and signal delay model accuracy

Figure S13: Wide circuit basal and activated RFP expression

Figure S14: Blue-light promoter characterization in CFS

Figure S15: Blue-light CRISPRi

Figure S16: EL222 titration in blue-light CRISPRa

Figure S17: Fusion orientation preference for SYNZIP and ABI/PYL1

Figure S18: Dependence of SYNZIP-CRISPRa on distance to TSS

Figure S19: Improvements in SYNZIP-CRISPRa from engineered promoters

Figure S20: Conditional CRISPRa scRNA dose-response

Figure S21: Comparisons of CRISPRa promoters to pTet

Figure S22: Three-layer activation cascade in *E. coli*

Supplementary Tables

Table S1: Promoters generated in this paper

Table S2: Dimerization domains affinity

Table S3: Primers for promoter mutagenesis

Table S4: Plasmids used in this work

Table S5: Deep cascades concentration

Table S6: Component sequences

Table S7: ANOVA analysis of combinatorial promoter screens

Supplementary Methods

Methods S1: Plasmid Preparation for Cell-Free System

Methods S2: CFS Blue-light CRISPRa/i modeling

Methods S3: Quantification and Statistical Analysis

Methods S4: Relationship between signal delay and signal propagation

Methods S5: Cell-Free Gene Expression Reactions

Methods S6: Plasmid and Library Construction

Methods S7: Optogenetic Illumination Setup

Methods S8: *E. coli* experiments culturing and quantification conditions

Methods S9: Plasmid and Library preparation

Methods S10: *E. coli* experiments

Methods S11: Design of promoter region libraries

Methods S12: Cell-free system preparation

Methods S13: Optogenetic experiments

Methods S14: CFS blue-light modeling

Methods S15: Quantification and statistical analysis

Supplementary Figures

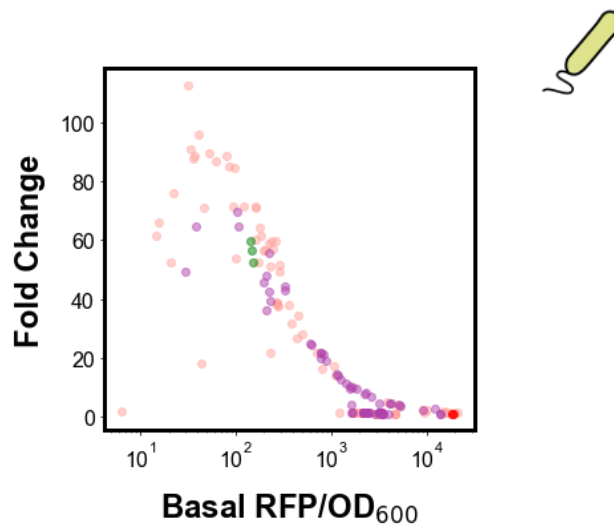


Figure S1: Minimal promoter effect on fold-change

Basal RFP/OD₆₀₀ and fold change for the two minimal promoter libraries ($n_{MP1} = 89$, $n_{MP2} = 84$). The J23117 minimal promoter (green, triplicates) is included as a standard reference for CRISPRa efficiency. The J23119 minimal promoter (red, triplicates) is an example of a non-activatable promoter due to high basal expression levels.

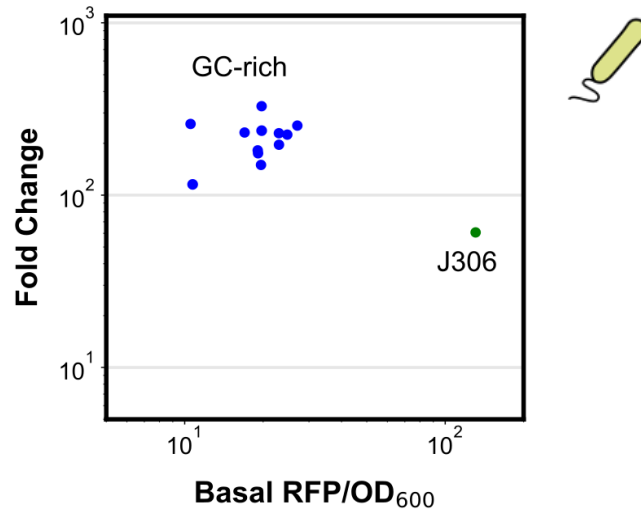


Figure S4: CRISPRa activity validation of high GC-content scRNAs

Fold change upon aTc induction and basal expression. scRNA target site sequences were initially selected based on low expression leak in *E. coli* and the corresponding scRNAs were constructed for use in CFS. Selected scRNAs were benchmarked against the standard J306 scRNA (green).

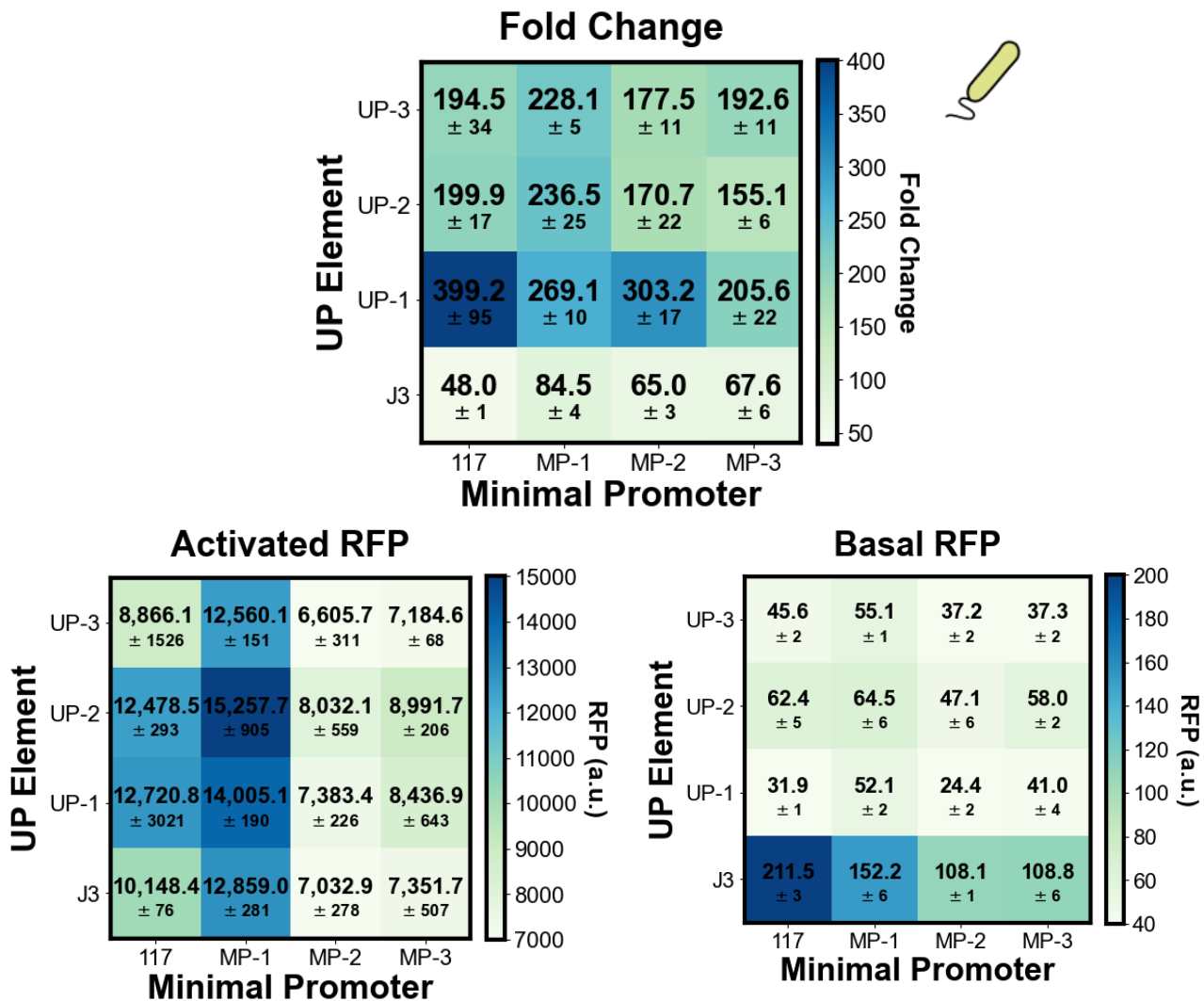


Figure S5: Combinatorial construction of activatable promoters

In addition to the J3.J23117 benchmark, three high performing variants each from the UP element and minimal promoter libraries were tested in a combinatorial manner for a total of 16 UP element/minimal promoter combinations screened in *E. coli*. We quantified the basal and activation expression of the 16 promoters with the same scRNA (bottom). Activation ratio is calculated by dividing the activated RFP expression from the inducible CRISPRa system by the basal RFP expression from each promoter (top). Values represent the mean ± standard deviation of three technical replicates.

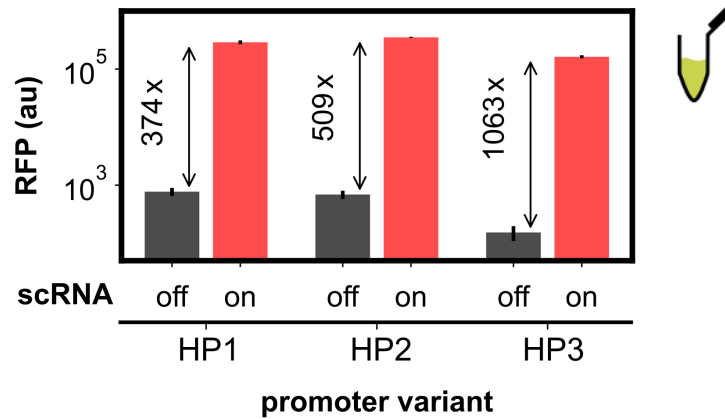


Figure S6: Activatable promoter characterization in CFS

Characterization of selected promoter variants in CFS. CRISPRa-mediated RFP expression levels (red, 0.4 nM scRNA DNA) and RFP basal expression levels (black, 0 nM scRNA DNA). Reactions contain 10 nM of RFP plasmid. Values represent the mean \pm standard deviation of three technical replicates.

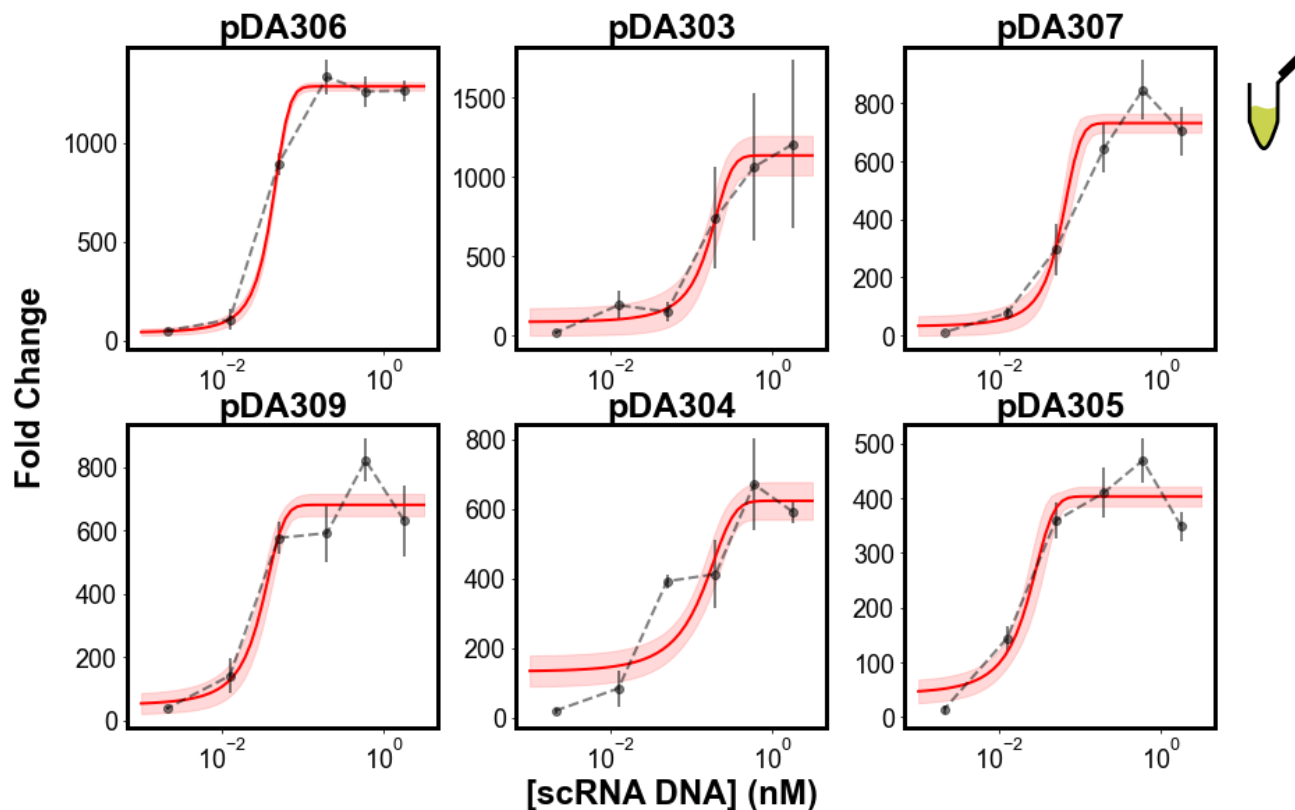


Figure S7: scRNA dose-response characterizations

scRNA dose-response curves are shown for orthogonal promoter-scRNA pairs in CFS. The scRNA-dose response curve is characterized through titrating the amount of scRNA DNA added to the CFS reaction. Reactions contain 10 nM of RFP plasmid. Red line indicates a logistic fit to the data. Values represent the mean \pm standard deviation of three technical replicates.

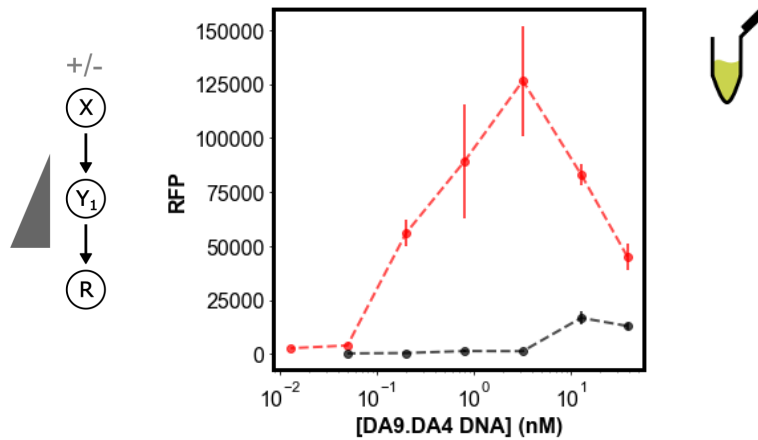


Figure S8: Titration of middle node in two-layer activation cascade

Two-layer activation cascade with high-performing components to identify the best performing internal node concentration. **Left:** Circuit schematic for measuring output RFP and fold change as a function of input scRNA. **Right:** Cascade RFP output with scRNA input (15 pM, red) and without (0 pM, black). Output node concentration is held constant at 10 nM. Values represent the mean \pm standard deviation of three technical replicates.

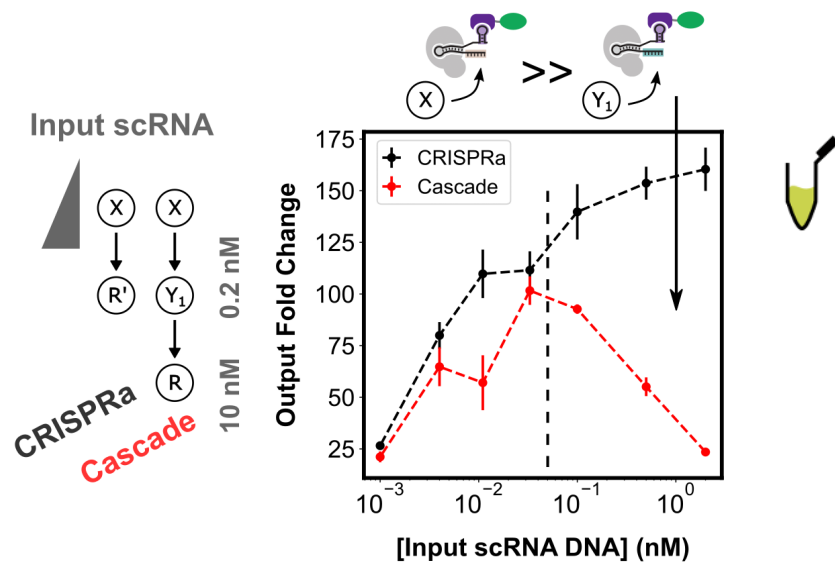


Figure S9: Signal propagation in a two-layer activation cascade

gRNA competition impact on circuit function. **Left:** Circuit schematic for measuring output fold change as a function of input scRNA for both CRISPRa (black) and CRISPRa cascade (red). Internal node concentration and output node concentration are held constant at 0.2 nM and 10 nM , respectively. **Right:** Input scRNA plasmid concentration was titrated between 1 pM and 2 nM . Black dashed line indicates saturation of CRISPRa complexes with input scRNA. Values represent the mean \pm standard deviation of three technical replicates.

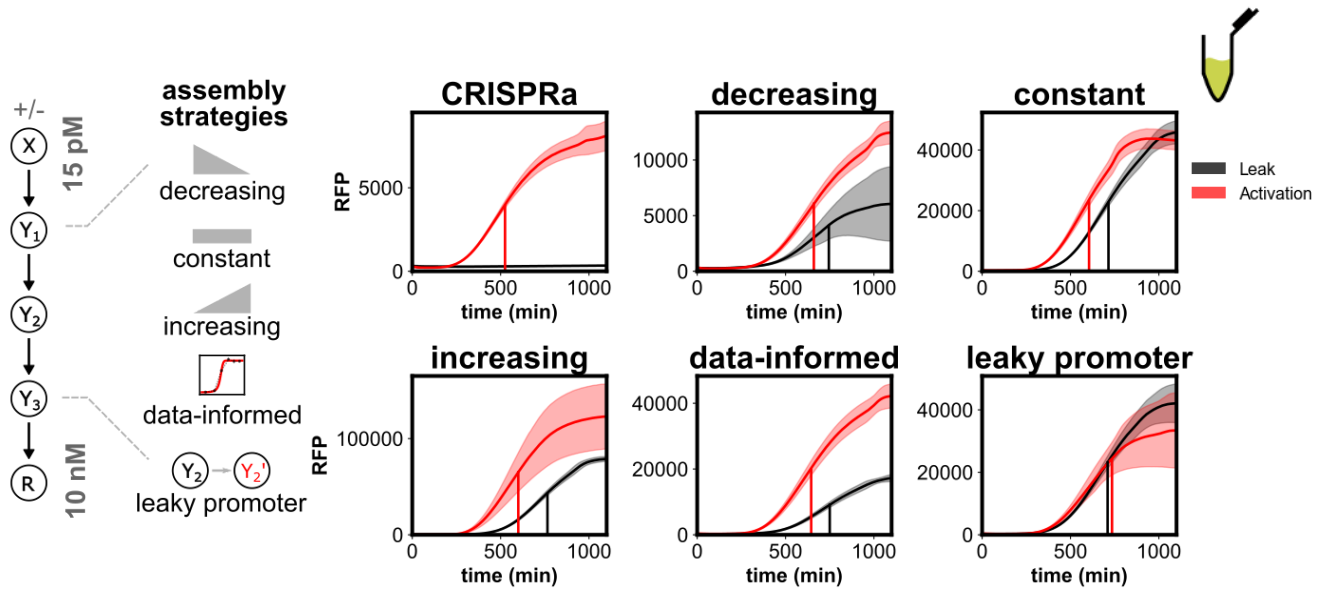


Figure S10: Time course for four-layer activation cascade assembly strategies

Comparison of the dynamics of four-layer CRISPRa cascade assemblies. **Left:** Internal node concentrations either decreased from 200 pM to 32 pM as depth increased, were held constant at 200 pM, or increased from 200 pM to 1.25 nM as depth increased. A fourth assembly method was tested in which internal node concentrations were 40, 200, and 170 pM, based on individual scRNA-dose response characteristics. A fifth cascade was included in which the high-performing promoter of the second internal node was replaced with the leaky J2 promoter. Input and output node concentrations were held constant across all strategies at 0 or 15 pM and 10 nM, respectively. **Right:** Output RFP expression for each assembly strategy with scRNA input (red) and without (black). Values represent the mean \pm standard deviation of three technical replicates. Time to maximum expression rate (t_{max}) for each assembly strategy is calculated by finding the time to reach maximum RFP production rate between (Methods 7.1).

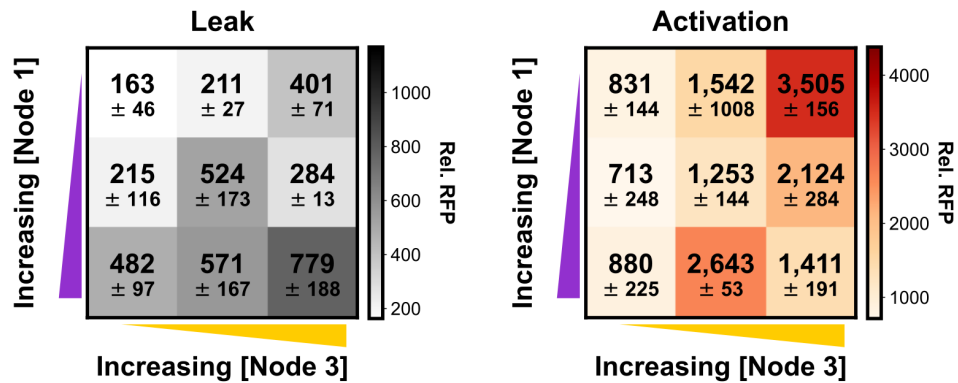


Figure S11: Four-layer activation cascade basal and activated RFP expression

Left: Basal expression levels for cascades titrating the first and third layers between 40 and 160 pM, and 85 and 340 pM, respectively. **Right:** Activated expression levels for the same cascades. The input node, second internal node, and output node were held constant at 0 or 15 pM, 0.2 nM, and 10 nM, respectively. Values are not background subtracted. Values represent the mean \pm standard deviation of three technical replicates.

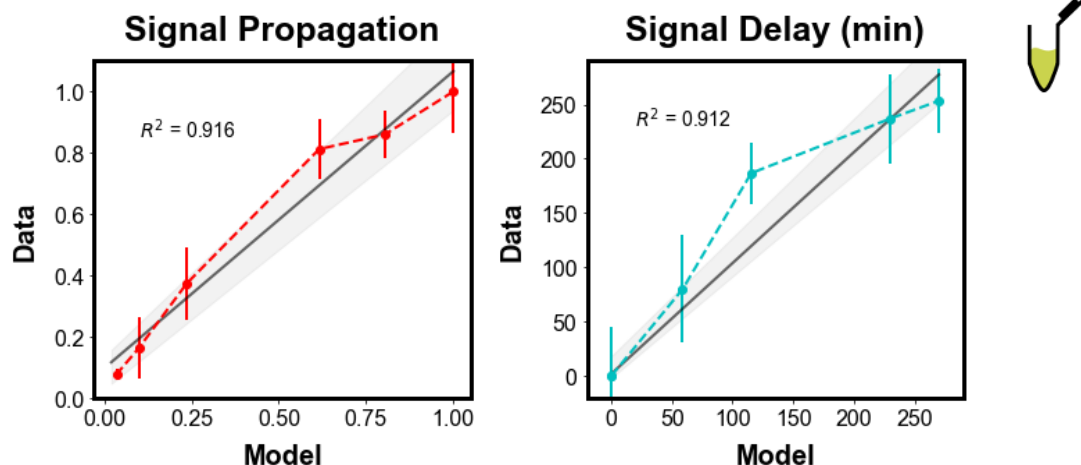


Figure S12: Signal propagation and signal delay model accuracy

Comparisons of measured and predicted signal propagation (left) and signal delay (right) for activation cascades of different depths. Signal propagation is calculated by dividing the fold-activation of the cascade output by the fold-activation from the input layer. (Methods 7.2). Signal delay is calculated as the difference between the cascade output and input layer in time to reach the maximum fold-activation (Methods 7.2). Both measures are presented as the mean \pm standard deviation of three technical replicates. The fold-change from the individual promoters' dose-response curves (Figure S7) are used to iteratively predict the delay and signal propagation at the next layer (Methods S4). Black line represents the mean \pm standard deviation of linear regression model measuring goodness-of-fit between model predictions and experimental data.

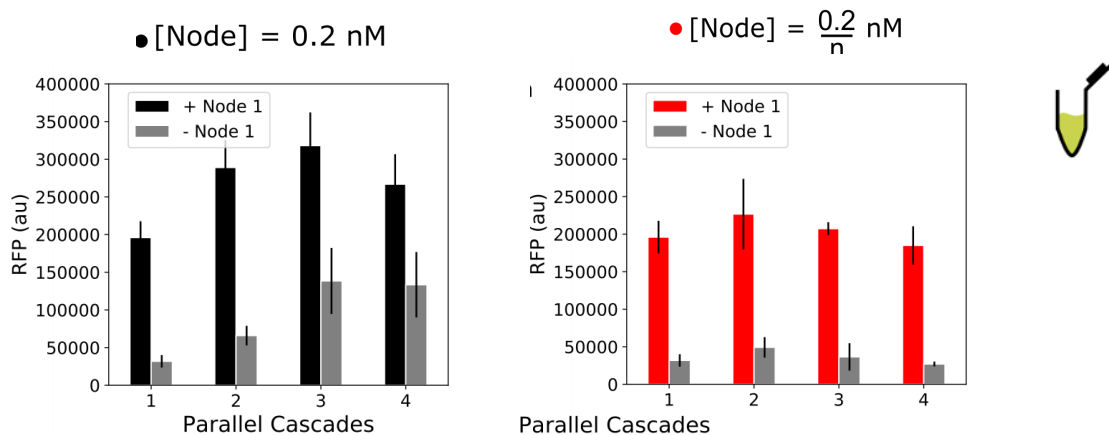


Figure S13: Wide circuit basal and activated RFP expression

Up to four parallel three-layer cascades were constructed. **Left:** The concentration of each internal node was held at 0.2 nM as circuit width increased. **Right:** The internal node concentration is scaled down proportionally to the width of the circuit, such that each internal node concentration is $0.2/n$ nM, where n is the number of parallel cascades.

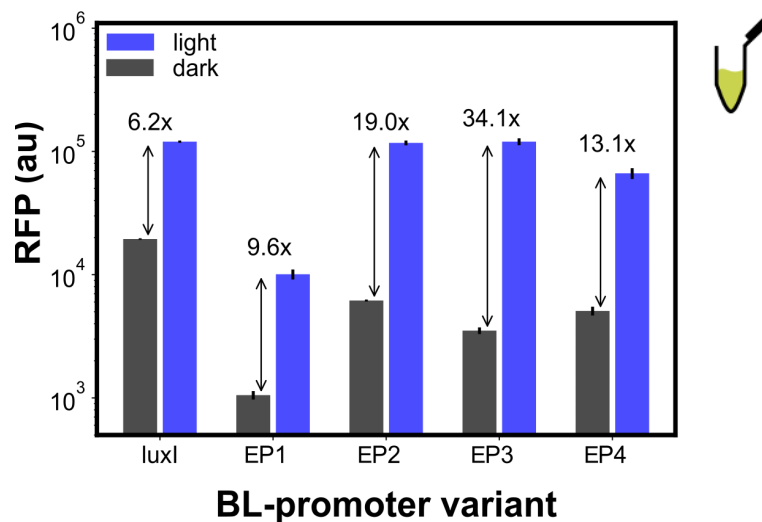


Figure S14: Blue-light promoter characterization in CFS

Characterization of selected promoter variants in CFS. Reactions contain 8 nM and 10 nM of EL222 and RFP plasmids respectively. EL222-mediated RFP expression levels (blue) and RFP basal expression levels (black). Values represent the mean \pm standard deviation of three technical replicates.

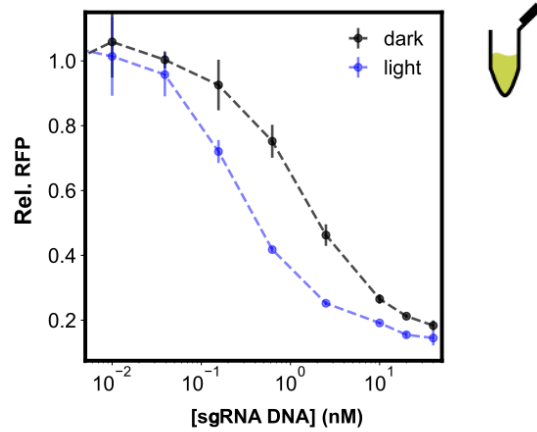


Figure S15: Blue-light CRISPRi

Titration of blue-light inducible sgRNA plasmid concentration to maximize the fold repression between blue-light dependent CRISPRi (blue) and CRISPRi due to sgRNA leak in the dark (black). Reactions contain 8 nM and 1 nM of EL222 and RFP plasmids respectively. Values represent the mean \pm standard deviation of three technical replicates.

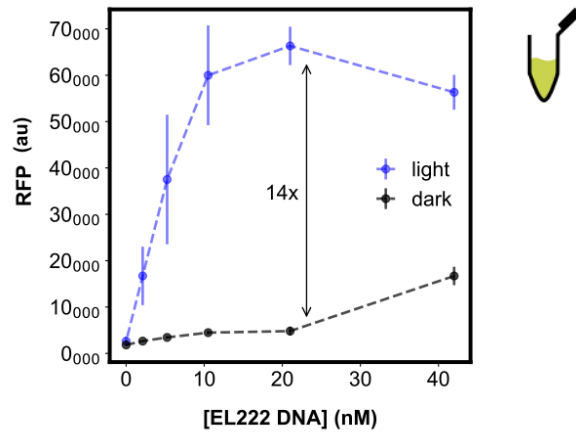


Figure S16: EL222 titration in blue-light CRISPRa

Titration of EL222 plasmid concentration to maximize the fold change between blue-light dependent CRISPRa (blue) and CRISPRa due to scRNA leak in the dark (black). Reactions contain 10 nM RFP plasmid. Values represent the mean \pm standard deviation of three technical replicates.

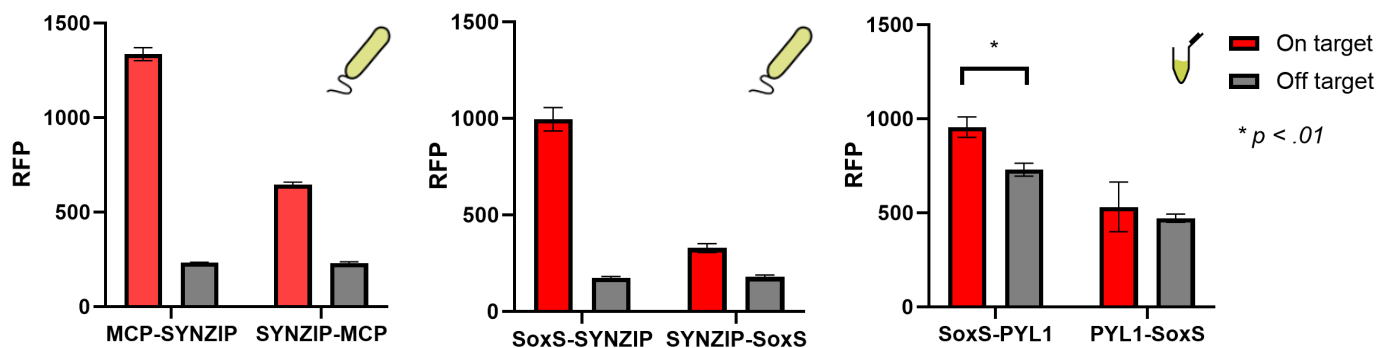


Figure S17: Fusion orientation preference for SYNZIP and ABI/PYL1

Left, Middle: MCP and SoxS fusion orientations were tested for the SYNZIP-CRISPRa system in *E. coli* using the J306 spacer at -81 bp from the TSS. The MCP test was done using SoxS-SYNZIP and the SoxS test was done using MCP-SYNZIP. **Right:** SoxS fusions were tested for the abscisic acid (ABA) CRISPRa system using MCP-ABI. The ABA constructs were tested in CFS using the R206 spacer at -81 bp from the TSS. ABA components were expressed at 5 nM. Off-target represents reactions containing a scRNA with no cognate target. Values represent the mean \pm standard deviation of three technical replicates.

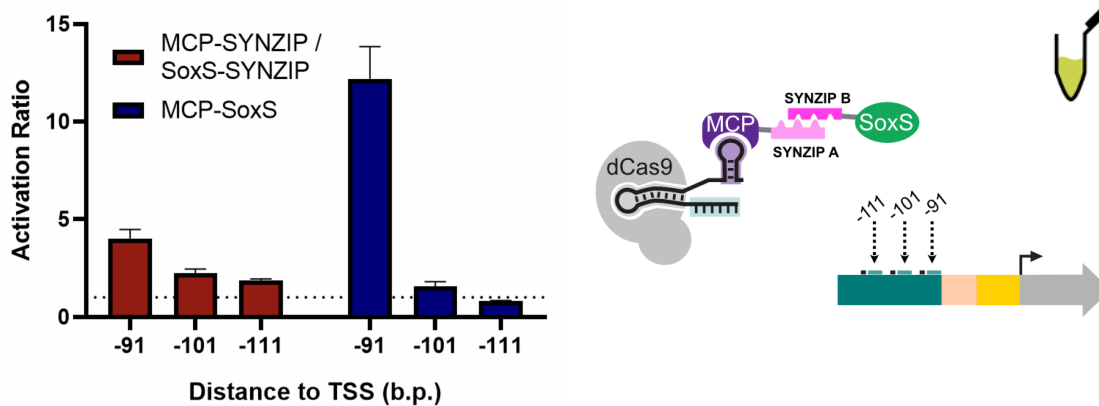


Figure S18: Dependence of SYNZIP-CRISPRa on distance to TSS

SYNZIP-CRISPRa and CRISPRa were tested at various target sites with increasing distance from the TSS in 10 bp intervals using a CRISPRa promoter with densely packed scRNA target sites. Plasmids expressing SYNZIP components are added at 5 nM each. Values represent the mean \pm standard deviation of three technical replicates.

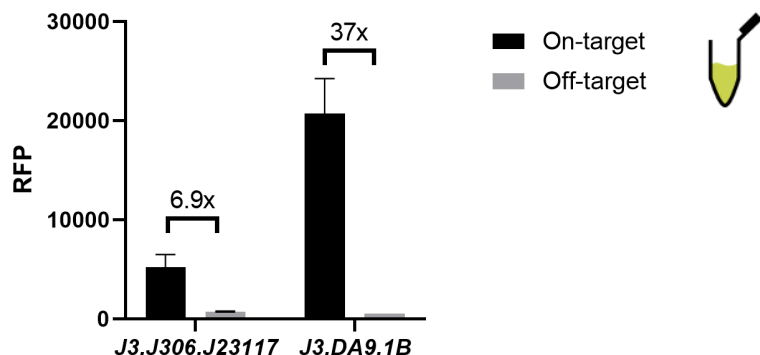


Figure S19: Improvements in SYNZIP-CRISPRa from engineered promoters

Comparison of SYNZIP-CRISPRa scRNA-dependent fold change with the previous synthetic promoter used to survey target sites and an engineered high dynamic range promoter. Off-target represents reactions containing a scRNA with no cognate target. In each reaction, the concentration of reporter DNA was 10 nM. SYNZIP components are added at 5 nM each. Reactions are background subtracted from a cell-free reaction containing no DNA. Values represent the mean \pm standard deviation of three technical replicates.

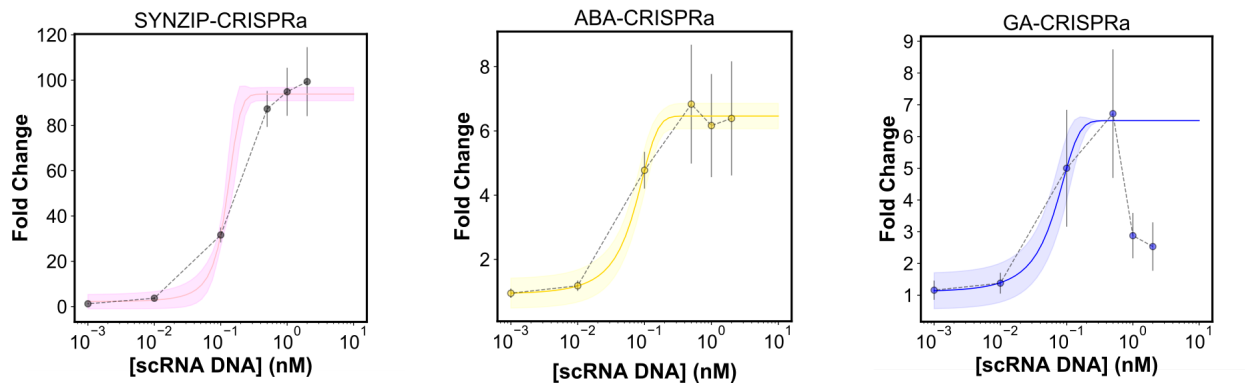


Figure S20: Conditional CRISPRa scRNA dose-response

scRNA-dose response curves were collected for conditional CRISPRa systems. scRNA concentrations were titrated between 10⁻³ and 10¹ nM. Fold activation was calculated relative to the no scRNA condition. For all conditions, ABA is added at 10 μM and GA is added at 10³ μM. SYNZIP-CRISPRa components were both added at 5 nM, MCP-ABI and SoxS-PYL1 were added at 5 and 10 nM respectively, and GA-CRISPRa components were both added at 10 nM. Colored lines indicate a logistic fit to the data. Values represent the mean ± standard deviation of three technical replicates.

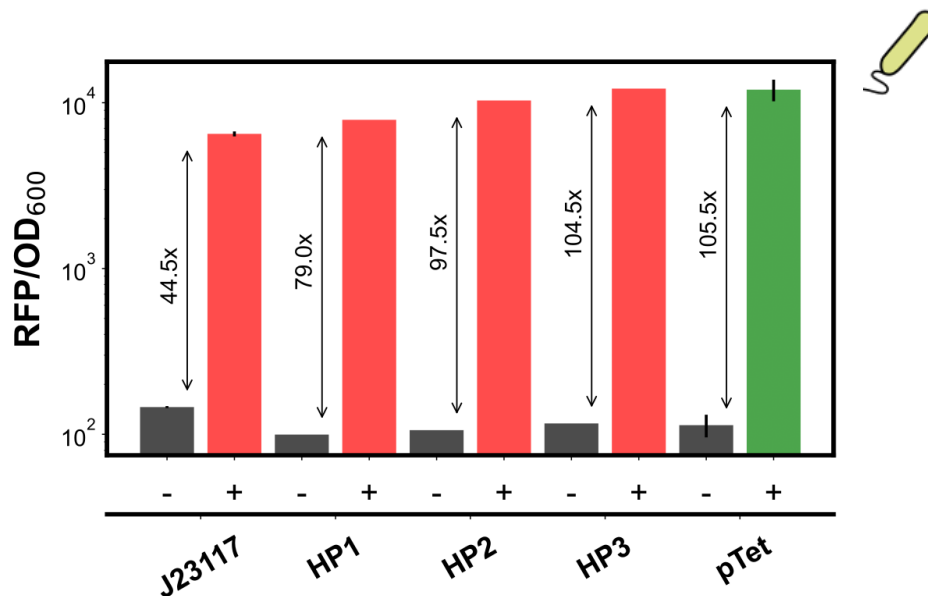


Figure S21: Comparison of CRISPRa promoters to pTet

Comparison of RFP expression levels of different CRISPRa promoters (red) to the pTet system (green). In both systems, RFP plasmid copy number and RBS remained constant. Basal expression level (“-”) is measured with off-target scRNAs for the CRISPRa promoters, and 0 nM aTc for pTet. Activated expression level (“+”) is measured with on-target scRNAs for the CRISPRa promoters, and 200 nM aTc for pTet. The J23117 and pTet values represent the mean \pm standard deviation of three technical replicates, whereas HP1-3 values correspond to the individual variants from the sequential screen (Figure 2D).

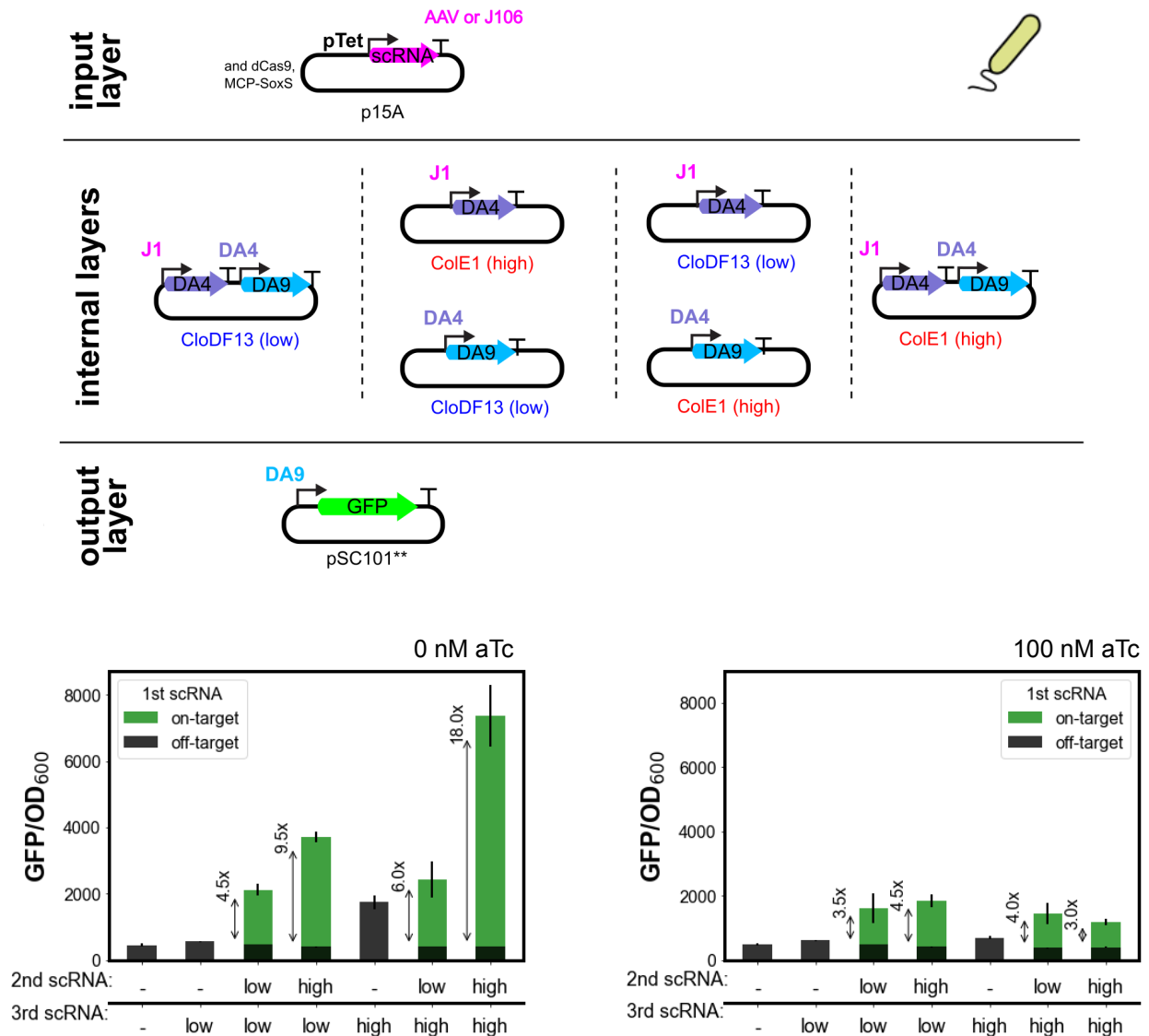


Figure S22: Three-layer activation cascades in *E. coli*

Three-layer activation cascades in *E. coli* with the input controlled by pTet and internal nodes expressed from different copy number plasmids. **Top:** Schematic of plasmids used for the different nodes. Input and output layers were kept constant across conditions, and the copy number of the plasmids encoding the two internal layers was varied between ColE1 (high copy) and CloDF13 (low copy). **Bottom, left:** GFP output for the different activation cascades at 0 nM aTc. Leak is minimized in the system when the third scRNA is expressed from a low copy number plasmid. Leak is also lowered when the second scRNA is present due to gRNA competition with the third scRNA.

Expressing the second scRNA from a high copy number resulted in higher fold-activation. **Bottom, right:** When induced with 100 nM aTc, cascade output is reduced, likely due to competition of the first scRNA with downstream scRNAs. Values represent the mean \pm standard deviation of three technical replicates

Supplementary Tables

Table S1: Promoters generated in this paper

Promoter	scRNA target	UP-element	Minimal Promoter	Basal	Activated
HP1_J3. DA9.2A	AACTCTCACA CGTGGCTGCA	CCGGCGGCGGCGG CTGCCGCGGCGG	TTGACAGTTTACGATGT GTTGGGATTGTGCTAGC	773.66 ± 123.99	289908.0 ± 22289.67
HP2_J3. DA9.1C	AACTCTCACA CGTGGCTGCA	CCGCGGGCGGCGG CTGCCGGGGCGG	TTGACACTTCCGGCACGA AAAGGGATTGTGCTAGC	690.33 ± 112.43	351826.66 ± 7551.20
HP3_J3. DA9.1B	AACTCTCACA CGTGGCTGCA	CCGCGGGCGGCGG CTGCCGGGGCGG	TTGACGCCTCCTTCTTTC TTAGGGATTGTGCTAGC	153.33 ± 43.81	163114.33 ± 10141.27
J3.DA2. 1B	CGCCGAATGC TCTAGCGGGA	CCGCGGGCGGCGG CTGCCGGGGCGG	TTGACGCCTCCTTCTTTC TTAGGGATTGTGCTAGC	567.33 ± 20.21	380117.0 ± 73224.73
J3.DA3. 1B	CACACCTAAG TCAGGATTGT	CCGCGGGCGGCGG CTGCCGGGGCGG	TTGACGCCTCCTTCTTTC TTAGGGATTGTGCTAGC	595.0 ± 39.05	279047.33 ± 14991.68
J3.DA4. 1B	CATATCTCTG ACCTGATCGA	CCGCGGGCGGCGG CTGCCGGGGCGG	TTGACGCCTCCTTCTTTC TTAGGGATTGTGCTAGC	263.66 ± 9.18	332795.33 ± 7755.96
J3.DA6. 1B	CACATAAAAA CCGCTGACTA	CCGCGGGCGGCGG CTGCCGGGGCGG	TTGACGCCTCCTTCTTTC TTAGGGATTGTGCTAGC	370.66 ± 40.35	313809.33 ± 15988.97
J3.DA9. 1B	AACTCTCACA CGTGGCTGCA	CCGCGGGCGGCGG CTGCCGGGGCGG	TTGACGCCTCCTTCTTTC TTAGGGATTGTGCTAGC	186.0 ± 79.92	224187.33 ± 20739.19
J3.DA10.1 B	AGAAACAGTA AAAACCTTCA	CCGCGGGCGGCGG CTGCCGGGGCGG	TTGACGCCTCCTTCTTTC TTAGGGATTGTGCTAGC	425.33 ± 29.86	349136.66 ± 15853.45
EP1	-	TCGGTAGCCTTTA GTCCATG	TTGACGCTGTATTCAGGC AAAGGGATTGTGCTAGC	1053.66 ± 82.92	10081.91 ± 940.10
EP2	-	TCGGTAGCCTTTA GTCCATG	TTGACAGTGCGTACGCAG GGAGGGATTGTGCTAGC	6170.33 ± 113.42	117299.0 ± 5279.40
EP3	-	TCGGTAGCCTTTA GTCCATG	TTGACGGTGAAGAGTATC AGAGGGATTGTGCTAGC	3516.66 ± 217.243	120075.33 ± 7740.25
EP4	-	TCGGTAGCCTTTA GTCCATG	TTGACAGCTCAGTGAGTA GTAGGGATTGTGCTAGC	5079.66 ± 417.91	66449.16 ± 6693.89
R2.E8. R206	(-81) TCGGCTCACT TATGCACGGC	CCGGCCCCCCCCG CTGCCGCGGGCCG	TTGACAAAGCTATGGCCG GCAGGGATTGTCACAGC	250.67 ± 21.2	6287.67 ± 670.47
R2.E8. R208	(-91) TCCCTGACCC TCGGCTCACT	CCGGCCCCCCCCG CTGCCGCGGGCCG	TTGACAAAGCTATGGCCG GCAGGGATTGTCACAGC	250.67 ± 21.2	3056.67 ± 414.77
R2.E8. R210	(-101) ACCCTTTCCT TCCCTGACCC	CCGGCCCCCCCCG CTGCCGCGGGCCG	TTGACAAAGCTATGGCCG GCAGGGATTGTCACAGC	250.67 ± 21.2	394.67 ± 56.89
R2.E8. R212	(-111) TTCCTCTCCT ACCCTTTCCT	CCGGCCCCCCCCG CTGCCGCGGGCCG	TTGACAAAGCTATGGCCG GCAGGGATTGTCACAGC	250.67 ± 21.2	206.67 ± 4.51

Table S2: Dimerization domain affinity

Domain	K _d	Method of measurement	Ref
MS2:MCP	.0033uM	Filter binding assay	(Carey et al., 1983)
SYNZIP5: SYNZIP6	<.015uM	Fluorescence polarization	(Thompson et al., 2012)
PYL1:ABA	1 - 52uM	Isothermal titration calorimetry, Surface plasmon resonance	(Dupeux et al., 2011; Miyazono et al., 2009)
PYL1:ABA:ABI	.030uM	Isothermal titration calorimetry	(Dupeux et al., 2011)
GID1:GA	.2 - 4uM	Radioactivity assay with isotopically labeled GA, <i>In vitro</i> FRET binding assay, Surface plasmon resonance	(Miyamoto et al., 2012; Ueguchi-Tanaka et al., 2005; Yoshida et al., 2018)
GAI:GA:GID1	.180uM	Surface plasmon resonance	(Yoshida et al., 2018)

Table S3: Primers for promoter mutagenesis

Minimal Promoter	
oMP1	CGATTATAGATTGACRGCTAGCTCAGTCCTDGNNAYNGTGCTAGCGAATTCATTAAAG AG
oMP2	CGATTATAGATTGACTTGACANNNNNNNNNNNNNAGGGATTGTNNNAGCGAATTCAT TAAAGAG
oMP3_S2	CGCTAGCACAATCCCWNNNNNSNNNNMRSYGTCAAGCCGGGAGAGCTGGTTCCATTG CGATTGCAGCCACGTGTGAGAGTT
oMP3_S2	CGCTAGCACAATCCCWNNNNNSNNNNMRSYGTCAACGCCGCCGCGCAGCCGGCGCGG GCGCTGCAGCCACGTGTGAGAGTT
oMP3_S2	CGCTAGCACAATCCCWNNNNNSNNNNMRSYGTCAACGCCGCGCGGCAGCCGCCGCCG

	CCGGTGCAGCCACGTGTGAGAGTT
UP-element	
oUP1	GCTAGCTGTCAAYNYTTTTTTAAAAAWWWWTNNNNNNTTGTGTCCAGAACGCTCCGT AG
oUP2	GCTAGCTGTCAAWWWWWWWWWWWWWWWWWWWWWWWWWTTGTGTCCAGAACGCTCCGT AG
oUP3	GCTAGCTGTCAAWWWHDWHDWHDWHDWHDWHDWHDWHDWHDWTTGTGTCCAGAACGCTCCGT AG
oUP4	GCTAGCTGTCAANNNNNNNNNNNNNNNNNNNNNNNNNNNTTGTGTCCAGAACGCTCCGT AG
oUP5	GCTAGCTGTCAABBBBSSSSBNNNNBSSSBSSSBSSSTTGTGTCCAGAACGCTCCGT AG
oUP6	GCTAGCTGTCAASSSSSSSSSSSSSSSSSSSSSSSSSTTGTGTCCAGAACGCTCCGT AG
oUP6_S1	GCTAGCTGTCAASSSSSSSSSSSSSSSSSSSSSSSSSTGCAGCCACGTGTGAGAGTT AG
scRNA target site	
oTS1	GCTCGTCTCCTCACTTCTCCTWWWWWWWWWWWWWWWWWWWWCCGGCCCCCCCCGCTGC CGCGGGCCGTTGACAGCTAGCTCAGTCCTAGG
oTS2	GCTCGTCTCCTCACTTCTCCTNNNNNNNNNNNNNNNNNNNNCCGGCCCCCCCCGCTGC CGCGGGCCGTTGACAGCTAGCTCAGTCCTAGG
oTS3	GCTCGTCTCCTCACTTCTCCTSSSSSSSSSSSSSSSSSSSSCCGGCCCCCCCCGCTGC CGCGGGCCGTTGACAGCTAGCTCAGTCCTAGG
EL222 promoter	
oMPE	CCTCTTTAATGAATTCGCTNNAACAATCCWNNNNNNSNNNNMRSYGTCAACATGGAC TAAAGGCTACCTATAAA

Table S4: Plasmids used in this work

Plasmid	J-Pro moter	scRNA target	UP Element	Minimal Promoter	RBS	CDS	gRNA	Terminator	res *	ori **
pJF143. J3	J3	J306	J3	J23117	Bujard	mRFP1	X	dbl term	A	S

pCK389. gRNA	X	X	X	Sp.Cas9, pTet, J23119	, Bujard, X	Sp.Cas9, MCP-Sox S (R93A,S1 01A)	J306, AAV, DA9	Dbl term, BBa_B1002, TrrnB	C	A
pJF182. gRNA	X	X	X	Sp.Cas9, J23107, J23119	, Bujard, X	Sp.Cas9, MCP-Sox S (R93A,S1 01A)	J306, AAV	dbl term, BBa_B1002, TrrnB	C	A
pDA010. 188	X	X	X	J23107	Bujard	Sp. dCas9	X	ECK120033 736	A	E
pRC029	X	X	X	J23107	Bujard	MCP-Sox S (R93A,S1 01A)	X	ECK120033 736	A	E
pRC011	X	X	X	J23107	Bujard	MCP-SY NZIP6	X	ECK120033 736	A	E
pRC012	X	X	X	J23107	Bujard	SoxS-SY NZIP5	X	ECK120033 736	A	E
pRC025	X	X	X	J23107	Bujard	MCP-ABI	X	ECK120033 736	A	E
pRC027	X	X	X	J23107	Bujard	SoxS-PY L1	X	ECK120033 736	A	E
pRC042	X	X	X	J23107	Bujard	MCP-GAI	X	ECK120033 736	A	E
pRC043	X	X	X	J23107	Bujard	SoxS-GI D1	X	ECK120033 736	A	E
pWS025 .BLNNN- RFP	X	X	X, EL222_Bi nding_re gion	J23119, N	BBa_B0 034, Bujard	EL222, mRFP1	X	BBa_B0015_ dblT, dbl term	A	S

pDA010. EL222	X	X	X	J23106	BBa_B0034	EL222	X	BBa_B0015_dbIT	A	E
pDA040. BLD7-mRFP	X	X	EL222_Binding_region	D7	X	mRFP1	X	ECK120033736	A	E
pDA040. BLD7-DA9	X	X	EL222_Binding_region	D7	X	X	DA9	ECK120033736	A	E
pDA040. BLD7-RR2	X	X	EL222_Binding_region	D7	X	X	RR2	ECK120033736	A	E
pDA303	J3	DA9	1	B	Bujard	mRFP1	X	ECK120033736	A	E
pDA304	J3	DA2	1	B	Bujard	mRFP1	X	ECK120033736	A	E
pDA305	J3	DA3	1	B	Bujard	mRFP1	X	ECK120033736	A	E
pDA306	J3	DA4	1	B	Bujard	mRFP1	X	ECK120033736	A	E
pDA307	J3	DA6	1	B	Bujard	mRFP1	X	ECK120033736	A	E
pDA309	J3	DA10	1	B	Bujard	mRFP1	X	ECK120033736	A	E
pDA310	J3	DA9	1	B	X	X	DA2	ECK120033736	A	E
pDA311	J3	DA9	1	B	X	X	DA3	ECK120033736	A	E
pDA312	J3	DA9	1	B	X	X	DA4	ECK120033736	A	E
pDA313	J3	DA9	1	B	X	X	DA6	ECK120033736	A	E

pDA314	J3	DA9	1	B	X	X	DA8	ECK120033 736	A	E
pDA315	J3	DA2	1	B	X	X	DA10	ECK120033 736	A	E
pDA316	J3	DA3	1	B	X	X	DA10	ECK120033 736	A	E
pDA317	J3	DA4	1	B	X	X	DA10	ECK120033 736	A	E
pDA318	J3	DA6	1	B	X	X	DA10	ECK120033 736	A	E
pDA319	J3	DA8	1	B	X	X	DA10	ECK120033 736	A	E
pDA320	J3	DA9	1	B	X	X	DA2	ECK120033 736	A	E
pDA321	J3	DA2	1	B	X	X	DA3	ECK120033 736	A	E
pDA322	J3	DA3	1	B	X	X	DA4	ECK120033 736	A	E
pDA323	J3	DA4	1	B	X	X	DA6	ECK120033 736	A	E
pDA324	J3	DA6	1	B	X	X	DA8	ECK120033 736	A	E
pDA325	J3	DA8	1	B	X	X	DA10	ECK120033 736	A	E
pRC014. (0-4)	R2	R206 (-81), R208 (-91), R210 (-101), R212 (-111)	E	8	Bujard	mRFP	X	ECK120033 736	A	E

pCK956. gRNA	X	X	X	J23107, J23107, pTet	Bujard, Bujard, X	Sp.Cas9, MCP-Sox S (R93A,S1 01A)	J106, AAV	Dbl term, BBa_B1002, TrmB	C	A
pDA506. gRNA	X	gRNA	1	B	Bujard	sfGFP	X	dbl term	K	S
pCK957	X	J106	1	B	X	X	DA4	Sht TermA	C, S	E, D
pCK958	X	J106, DA4	1	B	X	X	DA4, DA9	Sht TermA	C, S	E, D
pCK960	X	DA4	1	B	X	X	DA9	Sht TermA	C, S	E, D

*Resistance marker: C stands for chloramphenicol, A stands for ampicillin, S stands for spectinomycin, K stands for kanamycin

Origin of replication: E stands for ColE1, A stands for p15A, and S stands for sc101, and D stand for CloDF13

Table S5: Deep cascade concentrations

Cascade/ Plasmid	D1 -	D1 +	D2 -	D2 +	D3 -	D3 +	D4 -	D4 +	D5 -	D5 +	D6 -	D6 +
pDA010. 188	4	4	4	4	4	4	4	4	4	4	4	4
pRC029	4	4	4	4	4	4	4	4	4	4	4	4
pBT009.J1	0	.015	0	.015	0	.015	0	.015	0	.015	0	.015

.119.DA4												
pDA332			0.2	0.2	0.04	0.04	0.04	0.04	0.04	0.04	0.04	0.04
pDA320					0.2	0.2	0.2	0.2	0.2	0.2	0.2	0.2
pDA315							0.34	0.34	0.34	0.34	0.34	0.34
pDA335									0.13	0.13	0.13	0.13
pDA336											.093	.093
pDA306	10	10										
pDA303			10	10								
pDA304					10	10						
pDA309							10	10				
pDA307									10	10		
pDA305											10	10

All plasmid concentrations are in nM.

Table S6: Component sequences

pRC011: J23107.Buj.MCP-SYNZIP6

ttacggctagctcagccctaggtattatgctagcGAATTCATTAAAGAGGAGAAAGGTACCatggggccc
gcttctaactttactcagttcgttctcgtcgacaatggcggaaactggcgacgtgactgtcgcccaagcaactcgctaacgg
gatcgtgaatggatcagctctaactcgcgttcacaggcttacaagtaacctgtagcgttcgtcagagctctgcgcagaat
cgaaatacaccatcaaagtcgaggtgcctaaaggcgcctggcgttcgtacttaaatatggaactaaccattccaattttcg
ccacgaattccgactgcgagcttattgtaaggcaatgcaaggtctcctaaaagatggaaacccgattccctcagcaatcg
cagcaaaactccggcatctacGGTGGCGGAGGTAGCCAAAAAGTTGCGCAGCTGAAAAACCG
TGTTGCGTACAAACTGAAAGAAAACGCGAAGCTGGAGAACATCGTGGCGCGTCTG
GAAAACGACAATGCGAACCTGGAGAAAGACATTGCGAATCTCGAAAAGGACATCGC
AAATCTGGAACGTGACGTTGCGCGTTAAGCGGCCGCcacgcaaaaaaccccgttcggcggg
gtttttcgc

pRC012: J23107.Buj.SoxS-SYNZIP5

ttacggctagctcagccctaggtattatgctagcGAATTCATTAAAGAGGAGAAAGGTACCATGTCC
CATCAGAAAATTATTCAGGATCTTATCGCATGGATTGACGAGCATATTGACCAGCCGC
TTAACATTGATGTAGTCGCAAAAAAATCAGGCTATTCAAAGTGGTACTTGCAACGAAT
GTTCCGCACGGTGACGCATCAGACGCTTGGCGATTACATTCGCCAACGCCGCTG
TACTGGCCGCCGTTGAGTTGCGCACCACCGAGCGTCCGATTTTTGATATCGCAAT
GGACCTGGGTTATGTCTCGCAGCAGACCTTCTCCCGCGTTTTTCGCGCGGCAGTTT
GATCGCACTCCCGCGGATTATCGCCACCGCCTGGTGGCGGAGGTAGCAACACCG
TTAAAGAACTGAAAAACTACATCCAGGAGCTGGAAGAGCGTAACGCTGAACTCAA
AACCTGAAGGAACACCTGAAATTCGCAAAAGCGGAACTGGAATTCGAACTGGCGG
CTCACAAATTCGAGTAAGGCGCGCCcacgcaaaaaaccccgttcggcgggggttttttcgc

pRC025: J23107.Buj.MCP-ABI

tttacggctagctcagccctagggtattatgctagcGAATTCATTAAAGAGGAGAAAGGTACCatggggccc
gcttctaactttactcagttcgttctcgtcgacaatggcgggaactggcgacgtgactgtcgcccaagcaacttcgctaacgg
gatcgtgaatggatcagctctaactcgcgttcacaggcttacaagtaacctgtagcgttcgtcagagctctgcgcagaat
cgcaaatacaccatcaaagtcgaggtgcctaaaggcgcctggcgttcgtacttaaataatggaactaaccattccaatttcg
ccacgaattccgactgcgagcttattgtaaggcaatgcaaggtctcctaaaagatggaaacccgattccctcagcaatcg
cagcaaacctccggcatctacGGTGGCGGAGGTAGCACGCGTGTGCCTTTGTATGGTTTTACT
TCGATTTGTGGAAGAAGACCTGAGATGGAAGcTGCTGTTTCGACTATACCAAGATTC
CTTCAATCTTCCTCTGGTTCGATGTTAGATGGTCGGTTTGATCCTCAATCCGCCGCT
CATTCTTCGGTGTTCACGACGGCCATGGCGGTTCTCAGGTAGCGAACTATTGTAGA
GAGAGGATGCATTTGGCTTTGGCGGAGGAGATAGCTAAGGAGAAACCGATGCTCT
GCGATGGTGATACGTGGCTGGAGAAGTGGAAGAAAGCTCTTTTCAACTCGTTCCTG
AGAGTTGACTCGGAGATTGAGTCAGTTGCGCCGGAGACGGTTGGGTCAACGTCGG
TGGTTGCCGTTGTTTTCCCGTCTCACATCTTCGTCGCTAACTGCGGTGACTCTAGA
GCCGTTCTTTGCCGCGGCAAACTGCACTTCCATTATCCGTTGACCATAAACCGGAT
AGAGAAGATGAAGCTGCGAGGATTGAAGCCGCAGGAGGGAAAGTGATTCAGTGGA
ATGGAGCTCGTGTTTTCGGTGTTCTCGCCATGTCGAGATCCATTGGCGATAGATACT
TGAAACCATCCATCATTCTGATCCGGAAGTGACGGCTGTGAAGAGAGTAAAAGAA
GATGATTGTCTGATTTTGGCGAGTGACGGGTTTGGGATGTAATGACGGATGAAGA
AGCGTGTGAGATGGCAAGGAAGCGGATTCTCTTGTGGCACAAGAAAAACGCGGTG
GCTGGGGATGCATCGTTGCTCGCGGATGAGCGGAGAAAGGAAGGGAAAGATCCTG
CGGCGATGTCCGCGGCTGAGTATTTGTCAAAGCTGGCGATACAGAGAGGAAGCAA
AGACAACATAAGTGTGGTGGTGGTTGATTTGAAGTAAGGCGCGCCcaccgaaaaaacc
cgcttcggcgggggtttttcgc

pRC027: J23107.Buj.SoxS-PYL1

tttacggctagctcagccctagggtattatgctagcGAATTCATTAAAGAGGAGAAAGGTACCATGTCC
CATCAGAAAATTATTCAGGATCTTATCGCATGGATTGACGAGCATATTGACCAGCCGC
TTAACATTGATGTAGTCGCAAAAAAATCAGGCTATTCAAAGTGGTACTTGCAACGAAT
GTTCCGCACGGTGACGCATCAGACGCTTGGCGATTACATTCGCCAACGCCGCTG
TACTGGCCGCCGTTGAGTTGCGCACCACCGAGCGTCCGATTTTTGATATCGCAAT
GGACCTGGGTATGTCTCGCAGCAGACCTTCTCCCGGTTTTTCGCGCGGCAGTTT

GATCGCACTCCC GCGGATTATCGCCACCGCCTGGGTGGCGGAGGTAGC atgggtggg
gcgcgccaactcaagacgaattcacccaactctcccaatcaatcgccgagttccacacgtaccaactcggtaacggccg
ttgctcatctctcctagctcagcgaatccacgcgcccggaaacagtatggtccgtggtgagacgtttcgataggccaca
gattacaaacacttcatcaaaagctgtaacgtgagtgagatttcgagatgagtggtgacgcgcgacgtgaacg
tgataagtgattaccggcgaatacgtctcgagagagattagatctgttgacgatgatcggagagtgactgggttagtat
aacgggtggtgaacataggctgaggaattataaatcggttacgacggtcatagattgagaaagaagaagaaga
aaggatctggaccgtgtttggaatctatgttgtgatgtaccggaaggaattcggaggaagatacagattgttctgat
acggttattagattgaatcttcagaaaactgcttcgatcactgaagctatgaac TAAGCGGCCGCCcgcaaaaaac
cccgttcggcggggtttttcgc

pRC042: J23107.Buj.MCP-GAI

ttacggctagctcagccctagggtattatgctagc GAATTCATTAAAGAGGAGAAAGGTACC atggggccc
gcttctaactttactcagttcgttctcgtcgacaatggcggaaactggcgacgtgactgtcgcccaagcaacttcgctaacgg
gatcgtgaatggatcagctctaactcgcgttcacaggcttacaagtaacctgtagcgttcgtcagagctctgcgcagaat
cgaaatacaccatcaaagtcgaggtgcctaaaggcgcctggcgttcgtacttaaatatggaactaaccattccaattttcg
ccacgaattccgactcgcgagcttattgftaaggcaatgcaaggtctcctaaaagatggaaacccgattccctcagcaatcg
cagcaaaactccggcatctac GGTGGCGGAGGTAGCATGAAGCGCGATCATCATCACCACCA
CCACCAGGATAAAAAGACGATGATGATGAATGAGGAAGATGATGGAAACGGGATGG
ACGAATTGCTGGCAGTGCTGGGATATAAGGTGCGTTCGTCCGAAATGGCAGATGTT
GCTCAGAAATTGGAGCAGTTAGAAGTAATGATGAGTAACGTTCAAGAAGATGATCTT
TCACAGTTAGCGACCGAAACTGTCCACTACAACCCTGCTGAGCTTTACACTTGGTT
GGACTCCATGCTTACCGATCTTAACtgacgcaaaaaaccccgttcggcggggtttttcgc

pRC043: J23107.Buj.SoxS-GID1

ttacggctagctcagccctagggtattatgctagc GAATTCATTAAAGAGGAGAAAGGTACC ATGTCC
CATCAGAAAATTATTCAGGATCTTATCGCATGGATTGACGAGCATATTGACCAGCCGC
TTAACATTGATGTAGTCGCAAAAAAATCAGGCTATTCAAAGTGGTACTTGCAACGAAT
GTTCCGCACGGTGACGCATCAGACGCTTGGCGATTACATTCGCCAACGCCGCCTG
TTACTGGCCGCCGTTGAGTTGCGCACCACCGAGCGTCCGATTTTTGATATCGCAAT
GGACCTGGGTTATGTCTCGCAGCAGACCTTCTCCCGCGTTTTTCGCGCGGCAGTTT

GATCGCACTCCC GCGGATTATCGCCACCGCCTGGGTGGCGGAGGTAGCATGGCAG
CCTCCGACGAGGTAAATCTTATTGAGAGTCGTACCGTCGTTCCCTTGAATACTTGGG
TGTTGATCTCGAATTTCAAGGTCGCGTACAATATCTTACGCCGCCCGGATGGAACCT
TTAACCGTCACCTTGCAGAATATCTGGACCGCAAAGTTACAGCAAATGCTAATCCAG
TTGACGGTGTTCAGTTTTGACGTGCTGATTGATCGCCGTATCAACCTTCTGTCCC
GTGTCTATCGTCCTGCTTACGCCGATCAGGAGCAACCTCCATCCATTCTGGATCTG
GAAAAACCAGTGGATGGGGACATTGTCCCTGTCATCCTTTTTTTCCACGGGGGGTC
GTTCCGCCACTCGTCCGCCAACAGTGCGATCTACGACACTTTATGTCGTCGTCTTG
TCGGTCTTTGCAAATGCGTGGTCGTTTCCGTGAATTACCGTCGCGCTCCGGAGAAC
CCCTACCCATGTGCCTACGACGACGGATGGATTGCGTTAAATTGGGTAAATTCACGT
AGCTGGCTGAAAAGCAAGAAAGATTCTGAAGGTTACATTTTTTTAGCGGGCGATTCT
TCAGGAGGGAAACATCGCTCATAATGTCGCATTGCGTGCAGGAGAGTCTGGCATCGA
TGTTCTGGGCAACATTTACTGAACCCGATGTTTGGGGGAACGAGCGCACAGAAT
CCGAGAAAAGCTTGGACGGGAAGTATTCGTGACTGTTCCGCGATCGTGACTGGTAT
TGGAAGCGTTCTTGCCCGAGGGAGAGGACCGCGAGCACCCCGCATGCAACCCC
TTTTCACCTCGCGGAAAATCGCTGGAGGGGGTCAAGTTTCCCAAATCTTTAGTCGT
AGTAGCTGGCCTGGATCTGATCCGTGATTGGCAACTTGCGTATGCTGAAGGCCTTA
AGAAGGCTGGTCAAGAAGTAAAGCTGATGCACTTAGAGAAAGCTACGGTTGGCTTT
TATCTGTTACCAAATAACAATCACTTCCATAATGTGATGGATGAGATCTCCGCTTTCG
TTAATGCGGAATGCTgacgcaaaaaaccccgcttcggcggggtttttcgc

pDA010.EL222: J23106. BBaB0034.EL222

TTTACGGCTAGCTCAGTCCTAGGTATAGTGCTAGCCTAGAGAAAGAGGAGAAATACT
AGATGTTGGATATGGGACAAGATCGGCCGATCGATGGAAGTGGGGCACCCGGGGC
AGACGACACACGCGTTGAGGTGCAACCGCCGGCGCAGTGGGTCCTCGACCTGAT
CGAGGCCAGCCCGATCGCATCGGTGCGTGTCCGATCCGCGTCTCGCCGACAATCCG
CTGATCGCCATCAACCAGGCCTTACCGACCTGACCGGCTATTCCGAAGAAGAATG
CGTCGGCCGCAATTGCCGATTCTGGCAGGTTCCGGCACCGAGCCGTGGCTGAC
CGACAAGATCCGCCAAGGCGTGCGCGAGCACAAGCCGGTGCTGGTCGAGATCCT
GAACTACAAGAAGGACGGCACGCCGTTCCGCAATGCCGTGCTCGTTGCACCGATC
TACGATGACGACGACGAGCTTCTCTATTTCTCGGCAGCCAGGTCTGAAGTCGACGA

CGACCAGCCCAACATGGGCATGGCGCGCCGCGAACGCGCCGCGGAAATGCTCAA
GACGCTGTCGCCGCGCCAGCTCGAGGTTACGACGCTGGTGGCATCGGGCTTGCG
CAACAAGGAAGTGGCGGCCCGGCTCGGCCTGTCGGAGAAAACCGTCAAGATGCA
CCGCGGGGCTGGTGTATGGAAAAGCTCAACCTGAAGACCAGCGCCGATCTGGTGGC
CATTGCCGTCTGAAGCCGGAATCTAAGGATCCAACTCGAGTAAGGATCTCCAGGCA
TCAAATAAACGAAAGGCTCAGTCGAAAGACTGGGCCTTTCGTTTTATCTGTTGTTT
GTCGGTGAACGCTCTCTACTAGAGTCACACTGGCTCACCTTCGGGTGGGCCTTCT
GCGTTTATA

pDA040.BLD7-mRFP: EL222_Binding_region.D7.Bujard.mRFP

GGTAGCCTTTAGTCCATGTTGACGGTGAAGAGTATCAGAGGGATTGTGCTAGCGAA
TTCATTAAAGAGGAGAAAGGTACCATGGCGAGTAGCGAAGACGTTATCAAAGAGTT
CATgcgtttcaaagttcgtatggaaggtccggttaacgggtcacgagttcgaatcgaaggtgaaggtgaaggtcgccgt
acgaaggtaccagaccgctaaactgaaagttaccaaaggtggtccgctgccgttcgcttgggacatcctgtccccgcag
ttccagtacggttcaaagcttacgttaaacacccggctgacatcccggactacctgaaactgtcctcccgaaggttca
aatgggaacgtgttatgaacttcaagacggtggtgtgtaccgttaccaggactcctccctgcaagacggtgagttcatc
taciaagttaaactgcggtgtaccaaactcccgtccgacggtccggttatgcagaaaaaacatgggtgggaagcttcc
accgaacgtatgtaccggaagacggtgctctgaaaggtgaaatcaaatgctctgaaactgaaagacggtggtcact
acgacgctgaagttaaaaccacctacatggctaaaaaacgggtcagctgccgggtgcttcaaaaaccgacatcaaact
ggacatcacctcccacaacgaagactacaccatcggtgaacagtacgaacgtgctgaaggtcgtcactccaccggtgctt
aaggatccaaactcgagtaaggatctGTGCTTTTTTTTaaacgcatgagAAAGCCCCCGGAAGATCAC
CTCCGGGGGCTTTttattgcg

Table S7: ANOVA analysis of combinatorial promoter screens

	Sum of Squares	Degrees of Freedom	F Value	<i>p</i> Value
Minimal Promoter	23155.9	3	9.5	1.2e-4
UP-Element	315527.0	3	129.7	5.5e-18
Minimal Promoter & UP-Element	53678.2	9	7.4	1.0e-5
Residual	25954.2	32	-	-

Supplementary Methods

Methods S1: Plasmid Preparation for Cell-Free System

Plasmids intended for use in CFS were grown in culture volumes ~20 mL to ensure adequate yields for multiple cell-free reactions and were further purified using a PCR purification kit (Invitrogen PureLink, Cat. K310001), eluted into nuclease-free water. Plasmid concentrations were quantified via spectrophotometry (Nanodrop 2000c, Cat. ND-2000C).

Methods S2: CFS Blue-light CRISPRa/i modeling

The model was implemented using the text-based model definition language Antimony for Python 3.7. We introduced blue-light regulation as a piecewise function that modulates transcription of the sgRNA required for CRISPRi. We used linear functions of different slopes to capture the fast dimerization of the EL222 protein and binding to the DNA upon blight exposure as well as the slow unbinding in the absence of blue-light. Specifically, we the sgRNA basal transcription constant is modified with the following function:

$$\begin{aligned} & 0 \text{ if } 0 < t < t_{\text{delay}} \\ & \frac{k_{\text{max}}}{t_{\text{ON}}}(t - t_{\text{delay}}) \text{ if } t_{\text{delay}} < t < t_{\text{delay}} + t_{\text{ON}} \\ & k_{\text{max}} \text{ if } t_{\text{delay}} + t_{\text{ON}} < t < t_{\text{delay}} + t_{\text{ON}} + t_{\text{expose}} \\ & \frac{-k_{\text{max}}}{t_{\text{OFF}}}(t - (t_{\text{delay}} + t_{\text{ON}} + t_{\text{expose}})) \text{ if } t_{\text{delay}} + t_{\text{ON}} + t_{\text{expose}} < t < t_{\text{delay}} + t_{\text{ON}} + t_{\text{expose}} + t_{\text{OFF}} \end{aligned}$$

Where k_{max} represents the transcription rate constant when EL222 is fully bound to the promoter, and t_{delay} , t_{ON} , t_{expose} , and t_{OFF} represent the time delay for light exposure, the time for

EL222 dimerization and binding, the exposure time to light, and the time for EL222 unbinding upon removing the light source, respectively.

Methods S3: Quantification and Statistical Analysis

***E. coli* data analysis:**

Dynamic range:

Dynamic range was calculated as the ratio of measured RFP outputs without induction (0 nM aTc, or dark) and with induction (200nM aTc, or light):

$$DR = \frac{B^{\alpha_1} - B^0}{B^{\alpha_2} - B^0}$$

where:

B is RFP/OD₆₀₀ measured at endpoint

α_1 is activated expression, with induction

α_2 is basal expression, without induction

0 is no RFP expression

Pareto optimality:

To identify the best-performing promoter variants belonging to the Pareto front, we compared the basal and activated RFP expression levels of each variant to all other variants. A variant belongs to the Pareto front if no other variant had both lower basal and higher activated expression levels:

$$v_o \in P(V) \text{ if there is no } v \text{ such that } (v^a > v_o^a \ \& \ v^b < v_o^b) \text{ for all } v \in V$$

where:

V is the set of all promoter variants

v_o is a variant in V

v_o^a, v_o^b are the activated and basal expression levels of said variant

$P(V)$ is the set of promoter variants belonging to the Pareto front

Cell-free data analysis

Production Rate:

Throughout this work, we define production rate as:

$$\dot{B}^{\alpha}(t) = \frac{dB^{\alpha}}{dt} = \frac{B^{\alpha}(t+30) - B^{\alpha}(t)}{30}$$

where:

B is the measured RFP

α specifies the circuit topology and relevant plasmid concentrations

Relative Production Rates:

Relative production rates of CRISPRa mediated outputs were calculated as the ratio of CRISPRa mediated production rates divided by unregulated production rates. For CRISPRa the contribution due to unregulated basal expression was subtracted from measured output levels due to CRISPRa. This was done to isolate the timing of CRISPRa mediated gene expression from the comparatively early contribution of basal expression, and to allow observation of CRISPRa mediated gene expression dynamics under conditions where basal expression of reporter constructs dominates. Throughout this work, relative production rates are abbreviated as Rel. RFP Prod. Rate and are calculated as:

$$\dot{B}_{\Gamma}^{\alpha}(t) = \frac{\dot{B}^{\alpha}(t) - \dot{B}^{\Gamma}(t)}{\dot{B}^{\Gamma}(t)}$$

where:

α is a specific CRISPRa/i circuit

Γ is constitutive expression

Fold change:

Fold change was calculated as the ratio of RFP values generated by CRISPRa in the presence of input scRNA compared to RFP values generated in the absence of input scRNA.

$$FC^{\alpha}(y) = \frac{B^{\alpha+}(t) - B^{\Gamma}(t)}{B^{\alpha-}(t) - B^{\Gamma}(t)}$$

where:

$\alpha +$ is CRISPRa with y nM input scRNA

$\alpha -$ is CRISPRa without input scRNA

Γ is constitutive expression

Time to maximum expression rate:

To calculate the time to maximum expression rate, the contribution due to unregulated basal expression was subtracted from measured RFP levels due to CRISPRa. This was done to isolate the timing of CRISPRa mediated gene expression from the comparatively early contribution of leak, and to allow observation of CRISPRa mediated gene expression dynamics under conditions where basal expression of reporter constructs dominates. The time to maximum expression is denoted as t_{max} .

$$t = t_{max} \text{ when } \dot{B}_{\Gamma}^{\alpha}(t) = \max(\dot{B}_{\Gamma}^{\alpha}(t))$$

where:

α is a specific CRISPRa/i circuit

Γ is constitutive expression

Change in time to maximum expression rate (Δt_{max}) is calculated by finding the difference in time to reach maximum production rate between the with and without input conditions.

$$\Delta t_{max} = t_{max}^{\alpha+} - t_{max}^{\alpha-}$$

Signal propagation efficiency:

Propagation efficiency of the CRISPRa cascade in CFS was calculated as the maximum fold change in cascade output \pm input divided by the fold change provided by CRISPRa in the input layer at the same time point.

$$propagation = 100 \cdot \frac{\max(FC^{\alpha}(y))}{FC^{\beta}(y)}$$

where:

α is CRISPRa cascade with y nM of scRNAs

β is CRISPRa with y nM of scRNAs

Signal delay:

Signal delay is calculated as the difference in time to reach the maximum fold change of the cascade between the cascade output and input layer.

$$t^{\alpha} = t_{max}^{\alpha} FC \text{ when } FC^{\alpha}(y) = \max(FC^{\alpha}(y))$$

$$t^{\beta} = t_{max}^{\beta} FC \text{ when } FC^{\beta}(y) = \max(FC^{\beta}(y))$$

$$delay = t_{max}^{\beta} FC - t_{max}^{\alpha} FC$$

where:

α is CRISPRa cascade with y nM of scRNAs

β is CRISPRa with y nM of scRNAs

Methods S4: Relationship between signal delay and signal propagation

We define fraction of signal propagation at the n th node to be the product of the fraction of signal propagated at the previous nodes, namely:

$$fSP_n = \prod_i^n fSP_i$$

where the fraction of signal propagated by each node i is a function of the characteristic relative fold-change of node i , as well as the time of the reaction at which the signal propagates through node i :

$$fSP_i = rFC_i \cdot e^{-\frac{(\theta_i + t_o)}{\tau}}$$

where t_o is the reaction boot up time, and τ is the characteristic time of the system.

While seemingly simple, the exponential term accounts for the complex dynamics of cell-free expression and gRNA competition, and favors expression from earlier nodes.

The time of the reaction at which the signal propagates through the n th node can be estimated based on the fraction of the signal propagated through the n th node and the relative lifetime of the reaction:

$$\theta_n = rLT \cdot (1 - fSP_n)$$

where the relative lifetime of the reaction is the difference between the time to maximum fold activation of a one-layer cascade and the end of the reaction. With these equations and the characteristic relative fold-change of each node, both the signal delay and probation can be calculated iteratively.

Based on kinetic data, we set t_o and rLT to be ~2 hrs and ~5 hrs, respectively. In order to estimate τ , we fit the model to empirical signal propagation and delay data by minimizing the sum of residuals using the Nelder-Mead algorithm.

Methods S5: Cell-Free Gene Expression Reaction

Cell-free gene expression reactions were assembled on ice from the CFS and purified DNA. A master mix with common plasmids across reactions was prepared, and 1.5 μL per reaction allocated into PCR tubes. Plasmids which were varied across reactions were added in the remaining 1 μL . For reactions containing ABA (Sigma, A4906) or GA, .1 μL of the small molecules were added alongside the plasmids. For reactions involving more than 5 plasmids, plasmids were mixed with an acoustic liquid handler robot (Echo Labcyte 525). The CFS was pipette mixed and added to each PCR tube in 7.5 μL for a final volume of 10 μL . PCR tubes were vortexed, spun-down using a mini benchtop centrifuge, and placed on ice. Triplicates of 2.5 μL for each reaction were pipetted into individual wells of a 96-well V-bottom plate (Costar, Cat. 3363). The plate was sealed (Costar, Cat. 3080) and analyzed on a BioTek Synergy HTX plate reader at 29 $^{\circ}\text{C}$. mRFP1 fluorescence (ex. 540 nm, em. 600 nm) of cell-free reactions were measured every 10 min from the bottom of the plate. All reactions were run in batch mode.

Methods S6: Plasmid and Library Construction

All PCR amplification of plasmids and fragments used Phusion DNA polymerase in GC buffer. Primers were synthesized by IDT and resuspended into nuclease-free water. All PCR reactions were treated with DpnI for longer than 1 hour and purified using Qiagen gel extraction kits. Plasmid assembly was achieved using 5X In-Fusion HD mastermix (Takara).

Assembled plasmids and libraries were transformed into chemically competent NEB Turbo *E. coli* and plated onto LB-agar plates with either 100 $\mu\text{g}/\text{mL}$ carbenicillin or 25 $\mu\text{g}/\text{mL}$ chloramphenicol. Transformed cells were grown overnight ~16 hours at 37 $^{\circ}\text{C}$.

Single colonies were picked from plates and grown overnight in LB shaking at 37 °C with appropriate concentrations of relevant antibiotics.

Methods S7: Optogenetic setup

The samples were placed at 37 °C or 29 °C in an incubator (Thermo Forma Orbital Shaker, Model #435) with the illumination source placed atop the incubator and irradiating inwards. The distance between the illumination source and the *E. coli* deepwell plates was 14 cm. CFS reactions were placed inside the incubator at 29 °C at a distance of 6 cm with the bottom of the wells facing the illumination source. In both cases, the dark conditions were kept inside a cardboard box inside the incubator. Endpoint plate reader measurements were conducted using a BioTek Synergy HTX.

Methods S8: *E. coli* experiments culturing and quantification conditions

Transformed *E. coli* were outgrown for 1 hour shaking at 37 °C and plated onto LB-agar with carbenicillin and chloramphenicol. Plates were grown overnight at 37 °C. Experiments were conducted by picking three individual colonies into 400 µL Teknova EZ-RDM with 0.2% glucose and appropriate antibiotics in 96 well plates, covering with breathable membrane (Breathe Easier cat# Z763624) and shaking overnight at 37 °C at 1200 RPM on a Heidolph Titramax 1000. For inducible experiments, overnight cultures are subsequently diluted 1:40 into a fresh plate of EZ-RDM and supplemented with appropriate concentrations of aTc. Plate reader measurements were conducted using a BioTek Synergy HTX with a black flat bottom plate (Ref# 3631) using 100 µL of culture.

Methods S9: Plasmid and Library Preparation

Details regarding plasmid and library construction are presented in Methods S6. Plasmids were transformed into chemically competent NEB Turbo *E. coli*. 10 uL of the outgrowth with transformed libraries was diluted 1:20 with LB and plated onto LB-agar with carbenicillin to check library complexity. The remaining outgrowth was seeded into 5 mL of LB with carbenicillin or gentamicin. Cells were grown overnight ~16 hours at 37 °C. Single colonies were picked from plates and grown overnight in LB with carbenicillin. Single colonies and culture were sequence verified. Plasmids were isolated from subcultures using a DNA miniprep kit (QIAprep Spin Miniprep Kit) and Sanger sequenced (Genewiz inc.).

Methods S10: *E. coli* Experiments

dCas9, MCP-SoxS, and scRNA are on a p15A ori plasmid while reporter construct is located on a pSC101** ori plasmid. For experiments involving more than two plasmids, competent cells were first made from cells carrying the reporter plasmid and the CRISPRa plasmid (including either on- or off-target input scRNAs). The appropriate plasmids expressing internal scRNAs were transformed into the competent cells. Details regarding culturing conditions and quantification are provided in Methods S8.

Methods S11: Design of Promoter Region Libraries

3.1 Minimal Promoter Libraries: MP1 was designed by rationally mutagenizing specific bases that are known contacts of RNAP within the minimal promoter. MP2 was made by randomly mutagenizing within the intervening sequence. Since the libraries yielded similar Pareto fronts, we combined these mutations into MP3, used in the sequential screening process (Table S3).

3.2 UP-Element Libraries: We designed five UP-element libraries mutagenizing the AT-rich *E. coli* consensus sequence with increasing GC-content. We generated 5 libraries from 0% to 100% GC-content, and a library representing the *E. coli* consensus sequence (Table S3).

3.3 scRNA Target Site Libraries: We generated three scRNA target site libraries with varying compositions of GC-content (0%, 50%, and 100%) (Table S3). These libraries were used in tandem with a GC-rich UP-element.

3.4 EL222 Minimal Promoter Libraries: Starting with the native *luxI* minimal promoter, we introduced rational mutations to make it resemble a synthetic activatable promoter (J23117). We then randomly mutagenized within the -10:-35 region (Table S3).

Methods S12: Cell-Free System Preparation

CFS was acquired from Arbor Biosciences (myTXTL). The CFS used for an experiment was thawed on ice and pooled into a 1.5 ml Eppendorf tube, vortexed, and spun-down using a mini benchtop centrifuge to ensure sample homogeneity. Details about plasmid preparation are provided in Methods S1, and details about the CFS reaction are provided in Methods S5.

Methods S13: Optogenetic Experiments

E. coli cultures and CFS reactions were prepared as described above. The incubation conditions were modified to include a blue-light illumination source (UVP Visi-Blue UV Transilluminator, 8 Watts, 460/470 nm). Details about optogenetic setup are provided in Methods S7.

Methods S14: CFS Blue-light CRISPRa/i modeling

The CFS blue-light CRISPRa/i model was expanded from the previously described CFS CRISPRa/i model [32]. The model constitutes a series of first order chemical reactions for protein and guide RNA production, CRISPR complex assembly, and DNA targeting. All model details are described in Methods S2.

Methods S15: Quantification and statistical analysis

7.1 Data analysis: Throughout this work all measured RFP levels in *E. coli* were normalized by measured OD600 with appropriate propagation of uncertainties. All metrics are described in Methods S3.

7.2 Statistics: Statistical significance was calculated using two-tailed unpaired Welch's *t*-tests. Asterisks in Figures indicate a statistically significant difference (*: p-value < 0.05, **: p-value < 0.01, ***: p-value < 0.001).